IOP Conf. Series: Journal of Physics: Conf. Series **837** (2017) 012003 doi:10.1088/1742-6596/837/1/012003

Galactic cosmic ray propagation models using Picard

Ralf Kissmann
Leopold Franzens Universität Innsbruck, Austria
E-mail: ralf.kissmann@uibk.ac.at

Abstract. I will give an overview on the numerical approach for the solution of the Galactic cosmic-ray propagation problem used within the recently introduced code Picard. The code solves the transport equation for each cosmic-ray species resulting in a prediction of the cosmic ray flux everywhere in the Galaxy. Picard is a prominent example for the current transition from two-dimensional azimuthally symmetric models of Galactic cosmic-ray transport to those that allow higher degrees of realism. In Picard this is achieved by use of contemporary numerical solvers that allow efficient computation of very high resolution models. I will address the new physics that can be incorporated in such three-dimensional models, e.g. example problems like the transition from axisymmetric cosmic-ray source distributions to spiral-arm cosmic-ray source distributions, including consequences for the various observables related to cosmic rays.

1. Introduction

The majority of cosmic rays up to an energy of 10^{15} eV are thought to be of Galactic nature. They are accelerated by different sources and mechanisms all throughout the Galaxy (see (1) for a discussion of different sources). Here, our focus is on the transport of these particles throughout the Galaxy – to the observer at Earth. The transport of Galactic cosmic rays is determined by the interplay of several processes. Cosmic rays are subject to diffusion in space and also in energy due to scattering of the high-energy particles off irregularities in the interstellar magnetic field. They suffer from different kinds of energy-losses, where electrons are most severely affected. Additionally, heavy cosmic-ray nuclei can fragment in nuclear interactions with the interstellar gas. This is a loss process for the heavy nuclei and an additional secondary source process for lighter particles. In total, Galactic cosmic-ray transport is described by the following transport equation (see also 2; 3):

$$\frac{\partial \psi_i}{\partial t} = q(\vec{r},p) + \nabla\cdot\mathcal{D}\nabla\psi_i + \frac{\partial}{\partial p}p^2 D_{pp}\frac{\partial}{\partial p}\frac{1}{p^2}\psi_i - \nabla\cdot\vec{v}\psi_i - \frac{\partial}{\partial p}\left\{\dot{p}\psi_i - \frac{p}{3}(\nabla\cdot\vec{v})\psi_i\right\} - \frac{1}{\tau_f}\psi_i - \frac{1}{\tau_r}\psi_i. \quad (1)$$

This transport equations determines the cosmic-ray flux ψ_i for each cosmic-ray species i. In this equation, $q(\vec{r},p)$ describes the spatial distribution and the energy dependence of the cosmic-ray sources. $\mathcal{D}$ is the diffusion tensor, that can depend on energy, position and also direction in space. Similarly, D_{pp} is the momentum diffusion coefficient. Cosmic rays can be advected together with the interstellar gas moving with advection velocity $\vec{v}$. Additionally, $\dot{p}$ describes the energy losses and τ_f and τ_r are the time scales for fragmentation- or radiative losses, respectively.

Mathematically, the Galactic cosmic-ray transport equation is a four-dimensional diffusion-convection equation. Typically, the energy-dependence of the different terms in the cosmic-ray transport equation can be described as a power law in energy. This pertains in particular to

the energy dependence of the cosmic-ray source strength, the energy dependence of spatial- and momentum diffusion, and also the energy dependence of the different energy-loss rates. As a result the spectra of the different particle species are also of power-law form. However, the power-law index differs for different species and also in different energy regimes – depending on the relative importance of the transport parameters. Together with the wide range of energies relevant for Galactic cosmic-ray transport (ranging from hundreds up to some 10^9 MeV) the solution of this transport equation is numerically very demanding. In the following we will discuss available solution approaches in section 2 and, more in particular, the approach used in the PICARD code (4) in section 3. Finally, we present a few results in section 4.

2. Numerical solution of the cosmic-ray transport equation

For the numerical solution of the transport equation (1) there exist a range of numerical methods. These include grid-based methods, where the differential equation is solved by a discretisation in space, energy, and time, and a range of methods that propagate pseudo particles according to the prescription of the transport equation. The latter include Monte-Carlo-based methods as, e.g., discussed by (5) and also the use of so called stochastic differential equations (SDEs) (6; 7; 8). SDEs are particularly efficient in computing the cosmic-ray flux at a given position in space due to the possibility to perform a computation backwards in time – from the observer to the sources of cosmic rays. When, however, the distribution of cosmic rays everywhere in the Galaxy is of relevance, as for example in a study of Galactic diffuse emission (9), this method becomes computationally expensive. With a focus on methods suitable for the latter, we will only discuss grid-based solution methods of the cosmic-ray transport equation.

There are several Galactic cosmic-ray propagation codes available that rely on a grid-based solution method. These included, but are not limited to, DRAGON (10), GALPROP (11), and PICARD (4). The former two of these codes rely on a very similar numerical scheme: they use a dimensional splitting method for all spatial and the momentum dimension. For each dimensions the transport equation is discretised – typically using a Crank-Nicolson method – and the resulting tri-diagonal system of equations is solved via a standard method. The solution is then advanced in time according to a user-defined configuration of the given time-integration method.

Depending on the highest energy taken into account the characteristic time scales for Galactic cosmic-ray transport can become rather short - on the order of tens of years for cosmic-ray electrons. Additionally, the time until a converged solution is reached at <GeV energies, can be hundreds of millions of years. To avoid an extremely large number of time steps both schemes start the implicit time-integration scheme with a very large time step. Time-step size is then successively reduced until a smallest time step is reached that should reflect the characteristic time scale of the problem. For instance in GALPROP, however, the particular setup of the time-integration method is not controlled by the code but rather by the configuration file. While standard parameters for this setup usually yield satisfactory results, often the users are not aware of possible problems caused by an unsuitable choice of time-integration parameters (12). We found that sometimes also standard time-integration parameters can result in an error of up to ten percent in the cosmic-ray flux.

3. Steady-state solution scheme

Since the majority of studies relating to Galactic cosmic-ray transport focus on steady-state problems, i.e. problems where all transport parameters are time independent, the solution method applied by PICARD explicitly uses:

$$\frac{\partial \psi_i}{\partial t} = 0 \tag{2}$$

No time-integration is used in PICARD. Instead the transport equation is discretised in space and momentum only. This does not allow a dimensional splitting method as used in DRAGON and GALPROP any more, but leads to a system of algebraic equations with a band-diagonal matrix. In contrast to a tri-diagonal matrix there is no direct solution method available with a numerical cost of order $\mathcal{O}(N)$, where N is the number of coupled algebraic equations. Instead PICARD uses iterative methods to solve the system of equations. This does not yield an exact solution of the system of equations, but the iterations are stopped only when the residual is smaller than a threshold value that can be imposed by the user. The residual values reached by the code are smaller than the discretisation error. In the following we will describe the specifics of the solution approach in PICARD.

There are two types of steady-state solvers available in PICARD – depending on the transport-parameter setup. In Galactic cosmic-ray transport at least three types of propagation models are distinguished. In a so-called plain-diffusion model only spatial but no momentum diffusion is taken into account. In a reacceleration model also diffusive reacceleration or Fermi II acceleration is taken into account. In this case D_{pp} is non zero, effectively resulting in a diffusion in momentum space with an additional term describing an energy gain. In both these models spatial convection is often not taken into account. Thus, the third kind of models are such, where convection is additionally considered.

Apparently, in a plain-diffusion model without spatial convection, there is no term in the transport equation that can describe a possible energy gain. Cosmic rays are accelerated at the sources, resulting in a pre-defined source spectrum, and are thereafter only subject to spatial diffusion and energy losses. Also in a plain-diffusion model with non-zero convection fulfilling the condition $\nabla \cdot \vec{v} > 0$ everywhere there are no energy gains. This implies that the cosmic-ray flux at a given energy is independent from the flux at lower energies. This motivates the first numerical scheme used in PICARD, where the transport equation is solved successively at the different energy levels starting from the highest energy. At a given energy, the flux at the next-higher grid point in energy is used as input or initial condition and then only the spatial problem needs to be solved. By this the four-dimensional transport equation can be solved as a successive number of three-dimensional problems.

Regarding the numerical implementation this procedure is similar to a time-integration scheme, only that in PICARD we integrate from high to low energy. Ignoring spatial convection the transport equation in this particular case is:

$$-\nabla \cdot \mathcal{D}\nabla\psi_i + \frac{\partial}{\partial p}\left\{\dot{p}\psi_i\right\} + \frac{1}{\tau}\psi_i = q(\vec{r}, p), \tag{3}$$

where the time scales for fragmentation and radiative decay were combined into the decay time scale τ. Here, PICARD offers two principle sub-solvers. The first is analogous to a time-forward implicit discretisation of first order. For this an upwind finite-difference discretisation is used on the energy grid. The grid points are distributed as a power-law in energy, resulting in an equidistant representation when plotted logarithmically. After the discretisation in energy, at each energy level n a three-dimensional transport equation of the form:

$$-\nabla \cdot \mathcal{D}\nabla\psi_i\big|_n - \frac{\dot{p}\psi_i|_n}{p^{n+1} - p^n} + \left.\frac{\psi_i}{\tau}\right|_n = q(\vec{r}, p^n) - \frac{\dot{p}\psi_i|_{n+1}}{p^{n+1} - p^n} \tag{4}$$

is solved. For this Eq. 4 is discretised in space (currently, configuration space is discretised using finite differences on a Cartesian grid with constant grid spacings along each dimension) and then solved using an iterative method for band-diagonal matrices. In PICARD two solution methods are available for such band-diagonal matrices: a multigrid method (13) and a BiCGStab solver (14). For a model using spatially constant isotropic diffusion, the multigrid method is more

efficient, but for spatially-variable diffusion possibly with additional off-diagonal elements the BiCGStab method reaches a converged solution more quickly. The modular framework of the code also allows adding of additional solvers with relative ease.

For the multigrid solver different versions are implemented. For spatially constant, isotropic diffusion a simple red-black Gauss-Seidel method is very efficient. For anisotropic and possibly spatially variable diffusion an alternating plane solver is the preferred option.

The second sub-solver is second order in momentum. This is achieved by integrating Eq. (3) from p^n to p^{n+1}, which results in the alternative form for the energy-discrete transport equation:

$$-\nabla\cdot\mathcal{D}\nabla\psi_i|_n - \frac{2\dot{p}\psi_i|_n}{p^{n+1}-p^n} + \left.\frac{\psi_i}{\tau}\right|_n = \tilde{q}, \tag{5}$$

with

$$\tilde{q} = \nabla\cdot\mathcal{D}\nabla\psi_i|_{n+1} + q(\vec{r},p^n) + q(\vec{r},p^{n+1}) - \frac{2\dot{p}\psi_i|_{n+1}}{p^{n+1}-p^n} - \left.\frac{\psi_i}{\tau}\right|_{n+1}. \tag{6}$$

Here, the momentum integrals of all but the energy-loss term in Eq. (3) are evaluated via the trapozoidal rule, leading to the desired second-order behaviour even on the non-linear momentum grid. Eq. (5) is of the same principle form as Eq. (4) and can, thus, be solved using the same numerical scheme. This shows that the second order scheme is nearly identical in numerical cost, while offering higher precision – or the option to use fewer grid points in momentum.

Whenever energy gains are possible in a given configuration the plain-diffusion solver discussed above is not applicable any more. In that case a fully four-dimensional solver is used. Currently, the most efficient option in PICARD is using a four-dimensional multigrid solver. In this case the spatial derivatives are discretised in the same form as in the other schemes. Momentum derivatives are computed via finite differences on the power-law grid. For the usual three-point stencil this leads to first order behaviour for the energy-loss terms because central differencing is not suitable here, and an upwind discretisation needs to be used. As an alternative, PICARD also allows for a second-order discretisation of the energy-loss terms, by using a wider stencil.

At each multigrid level all three-dimensional sub problems at even momentum grid points and then those at odd momentum grid points are solved. In that regard the approach is similar to the red-black Gauss-Seidel solver. For the solution of the corresponding three-dimensional sub-problems at given momenta we apply the same three-dimensional solvers as for the plain-diffusion form of the transport equation.

Here, we described the specific solvers for the transport equation of a single cosmic-ray species. Due to radioactive decay and fragmentation reactions different species can interact with each other. This interaction is realised by the loss-terms and the source term in Eq. (1). To acknowledge the coupling of the different cosmic-ray species, the transport equation for the heaviest nucleus with the highest charge is solved first. Then the transport equations for the lighter nuclei are solved successively. Whenever a nucleus is treated that can decay into one that was addressed earlier in this nuclear reaction network, and can thus contribute to its source function, the transport equation for the earlier nucleus is solved again. Thus, the part of the nuclear network between the two coupled species is iterated several times. In (12) we discuss further details of this implementation and show that usually two such iterations are sufficient to lead to a converged result.

All solvers have been verified by being applied to a range of analytically solvable problems in (4). Additionally, results produced with other codes have successfully been reproduced using PICARD, as, e.g., shown in (12). PICARD is fully MPI parallel and has been run on distributed- and shared-memory machines successfully. By construction and due to its efficiency, PICARD is particularly suited for the solution of three-dimensional propagation problems, where in the

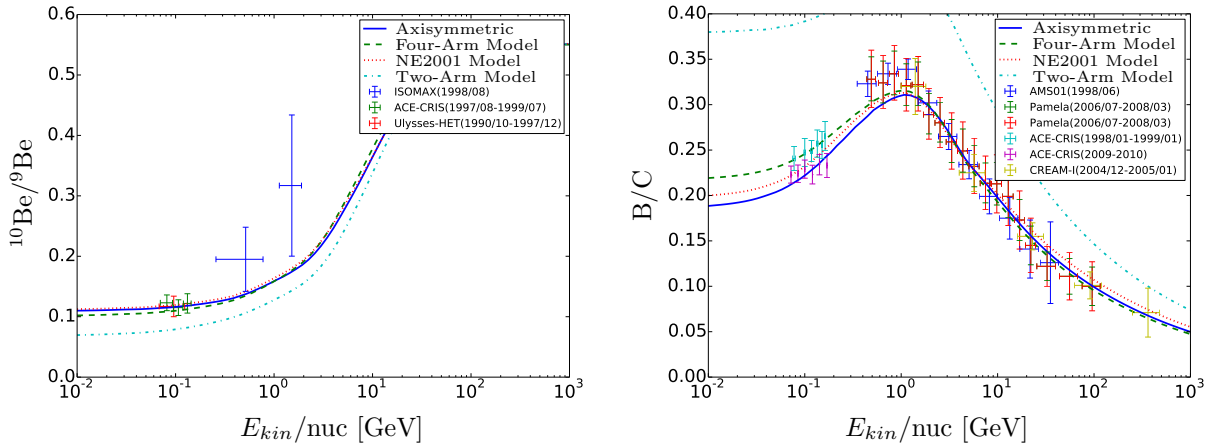

Figure 1. Secondary to primary ratios for a range of spiral-arm source-distribution models in the context of Galactic cosmic-ray transport. On the left we show results for the ^{10}Be to ^{9}Be ratio and on the right for the total Boron to total Carbon ratio.

past often axisymmetric setups were used for the Galaxy (see, e.g. 3) applying a two-dimensional setup using cylindrical coordinates.

4. Example results

Due to the optimisation for the solution of spatially three-dimensional problems, PICARD has been applied to the Galactic cosmic-ray transport problem under the assumption that the sources of cosmic rays are concentrated along the Galactic spiral arms. This has lately also been addressed by other groups (5; 8; 15; 16; 7). Such a source distribution is motivated by cosmic rays being supposedly accelerated predominantly at young astrophysical objects like, e.g., supernova remnants and pulsar-wind nebulae.

In (17) we investigated the impact of different such localised source distributions on the proton and electron flux at different energies, which are the most relevant species for the Galactic diffuse gamma-ray emission (9). In a follow-up study (12) we verified that a set of propagation parameters can be found by which also models using a localised source distribution yield a good fit to cosmic-ray fluxes observed at Earth.

Corresponding results for the resulting secondary-to-primary ratios are shown in Fig. 1 where propagation parameters as discussed in (12) are used. In this case we investigated an axisymmetric source distribution model taken from (9), a model with a logarithmic four-arm source distribution model extracted from (18, the four-arm Model), a source distribution model based on the parametrisation by (19, the NE2001-Model) and a two-arm model with a Galactic bar based on (20). The ^{10}Be/^{9}Be ratio and the B/C ratio shown in Fig. 1 are the best measured of the secondary-to-primary ratios, allowing to judge the quality of a fit – especially since they do not show a power-law distribution in energy. Another interesting constraint for the propagation physics is the measured antiproton flux, but reproducing these measurements can still be problematic (see, e.g., 21). For this, an investigation of the impact of the more recent presciption for the antiproton production cross section by (22) will be interesting. This cross section has been a recent addition to the PICARD code.

For the four-arm Model and the NE2001 model we found a satisfactory agreement with observations at Earth. For the two-arm Model, however, it was so far not possible to find a set of transport parameters that could describe the observations with convincing values for the different parameters (see also 23). It turns out, however, that the quality of the fit is mostly

determined by the sources nearest to the Earth, where the two-arm model suffers from the nearest spiral arms not being taken into account in that case. However, when adding the local spiral-arm segment near Earth to the model, also the two-arm model should be able to reproduce the observations (see 12).

This shows that very different source-distribution models can lead to a good fit to observational data - despite very different spatial distributions of the cosmic-ray flux. As mentioned above, this is because the observable flux at Earth is predominantly determined by the nearest cosmic-ray sources. This also means that the diffuse gamma-ray emission should be rather different in the different models, since it originates everywhere in the Galaxy – this is currently being studied using PICARD. Apart from that, the results also show the applicability of PICARD to studies of fully three-dimensional transport problems of Galactic cosmic rays.

5. Conclusions

Here, we discussed the specific implementation of the numerical solution scheme used in the PICARD code to solve the Galactic cosmic-ray transport problem. We focussed on the implementation of the different steady-state solvers in PICARD, although there is also a time-evolution scheme for time-dependent cosmic-ray transport problems. PICARD has successfully been applied to transport problems with localised source distributions, where a few results have been discussed, here. Current developments in PICARD include the application of spatially variable diffusion using a full diffusion tensor and the implementation of a new interstellar radiation field. The latter will be particularly important in a study of the Galactic center physics. For this relevant constraints will mostly come from diffuse gamma-ray emission, because the cosmic-ray flux at Earth is mostly determined by near-by sources.

References

[1] Aharonian F, Akhperjanian A G, Bazer-Bachi A R, Beilicke M, Benbow W, Berge D, Bernlöhr K, Boisson C, Bolz O, Borrel V, Braun I, Breitling F, Brown A M, Chadwick P M, Chounet L M, Cornils R, Costamante L, Degrange B, Dickinson H J, Djannati-Ataï A, Drury L O, Dubus G, Emmanoulopoulos D, Espigat P, Feinstein F, Fontaine G, Fuchs Y, Funk S, Gallant Y A, Giebels B, Gillessen S, Glicenstein J F, Goret P, Hadjichristidis C, Hauser M, Heinzelmann G, Henri G, Hermann G, Hinton J A, Hofmann W, Holleran M, Horns D, Jacholkowska A, de Jager O C, Khélifi B, Komin N, Konopelko A, Latham I J, Le Gallou R, Lemière A, Lemoine-Goumard M, Leroy N, Lohse T, Martin J M, Martineau-Huynh O, Marcowith A, Masterson C, McComb T J L, de Naurois M, Nolan S J, Noutsos A, Orford K J, Osborne J L, Ouchrif M, Panter M, Pelletier G, Pita S, Pühlhofer G, Punch M, Raubenheimer B C, Raue M, Raux J, Rayner S M, Reimer A, Reimer O, Ripken J, Rob L, Rolland L, Rowell G, Sahakian V, Saugé L, Schlenker S, Schlickeiser R, Schuster C, Schwanke U, Siewert M, Sol H, Spangler D, Steenkamp R, Stegmann C, Tavernet J P, Terrier R, Théoret C G, Tluczykont M, Vasileiadis G, Venter C, Vincent P, Völk H J and Wagner S J 2006 *ApJ* **636** 777–797 (*Preprint* `astro-ph/0510397`)

[2] Parker E N 1965 *Planet. Space Sci.* **13** 9–49

[3] Strong A W, Moskalenko I V and Ptuskin V S 2007 *Annual Review of Nuclear and Particle Science* **57** 285–327 (*Preprint* `arXiv:astro-ph/0701517`)

[4] Kissmann R 2014 *Astroparticle Physics* **55** 37–50 (*Preprint* `1401.4035`)

[5] Benyamin D, Nakar E, Piran T and Shaviv N J 2014 *ApJ* **782** 34 (*Preprint* `1308.1727`)

[6] Zhang M 1999 *ApJ* **513** 409–420

[7] Kopp A, Büsching I, Potgieter M S and Strauss R D 2014 *New Astronomy* **30** 32–37

[8] Effenberger F, Fichtner H, Scherer K and Büsching I 2012 *A&A* **547** A120 (*Preprint* `1210.1423`)

[9] Ackermann M, Ajello M, Atwood W B, Baldini L, Ballet J, Barbiellini G, Bastieri D, Bechtol K, Bellazzini R, Berenji B, Blandford R D, Bloom E D, Bonamente E, Borgland A W, Brandt T J, Bregeon J, Brigida M, Bruel P, Buehler R, Buson S, Caliandro G A, Cameron R A, Caraveo P A, Cavazzuti E, Cecchi C, Charles E, Chekhtman A, Chiang J, Ciprini S, Claus R, Cohen-Tanugi J, Conrad J, Cutini S, de Angelis A, de Palma F, Dermer C D, Digel S W, Silva E d C e, Drell P S, Drlica-Wagner A, Falletti L, Favuzzi C, Fegan S J, Ferrara E C, Focke W B, Fortin P, Fukazawa Y, Funk S, Fusco P, Gaggero D, Gargano F, Germani S, Giglietto N, Giordano F, Giroletti M, Glanzman T, Godfrey G, Grove J E, Guiriec S, Gustafsson M, Hadasch D, Hanabata Y, Harding A K, Hayashida M, Hays E, Horan D, Hou X, Hughes R E, Jóhannesson G, Johnson A S, Johnson R P, Kamae T, Katagiri H, Kataoka J, Knödlseder J, Kuss M, Lande J, Latronico L, Lee S H, Lemoine-Goumard M, Longo F, Loparco F, Lott B, Lovellette M N, Lubrano P, Mazziotta M N, McEnery J E, Michelson P F, Mitthumsiri W, Mizuno T, Monte C, Monzani M E, Morselli A, Moskalenko I V, Murgia S, Naumann-Godo M, Norris J P, Nuss E, Ohsugi T, Okumura A, Omodei N, Orlando E, Ormes J F, Paneque D, Panetta J H, Parent D, Pesce-Rollins M, Pierbattista M, Piron F, Pivato G, Porter T A, Rainò S, Rando R, Razzano M, Razzaque S, Reimer A, Reimer O, Sadrozinski H F W, Sgrò C, Siskind E J, Spandre G, Spinelli P, Strong A W, Suson D J, Takahashi H, Tanaka T, Thayer J G, Thayer J B, Thompson D J, Tibaldo L, Tinivella M, Torres D F, Tosti G, Troja E, Usher T L, Vandenbroucke J, Vasileiou V, Vianello G, Vitale V, Waite A P, Wang P, Winer B L, Wood K S, Wood M, Yang Z, Ziegler M and Zimmer S 2012 *ApJ* **750** 3

[10] Evoli C, Gaggero D, Grasso D and Maccione L 2008 *J. Cosmology Astropart. Phys.* **10** 18 (*Preprint* 0807.4730)

[11] Strong A W and Moskalenko I V 1998 *ApJ* **509** 212–228 (*Preprint* arXiv:astro-ph/9807150)

[12] Kissmann R, Werner M, Reimer O and Strong A W 2015 *Astroparticle Physics* **70** 39–53 (*Preprint* 1504.08249)

[13] Trottenberg U, Osterlee C and Schuller A 2001 *Multigrid* (Orlando, FL, USA: Academic Press, Inc.) ISBN 0-12-701070-X

[14] Sleijpen G L and Fokkema D R 1993 *Electronic Transactions on Numerical Analysis* **1** 2000

[15] Jóhannesson G, Moskalenko I V and Porter T 2013 *Proceedings of the 33rd International Cosmic Ray Conference*

[16] Jóhannesson G, Moskalenko I V, Orlando E, Porter T and Strong A W

[17] Werner M, Kissmann R, Strong A W and Reimer O 2015 *Astroparticle Physics* **64** 18–33 (*Preprint* 1410.5266)

[18] Steiman-Cameron T Y, Wolfire M and Hollenbach D 2010 *ApJ* **722** 1460–1473

[19] Yusifov I and Küçük I 2004 *A&A* **422** 545–553 (*Preprint* astro-ph/0405559)

[20] Dame T M and Thaddeus P 2011 *ApJ* **734** L24 (*Preprint* 1105.2523)

[21] Jóhannesson G, Ruiz de Austri R, Vincent A C, Moskalenko I V, Orlando E, Porter T A, Strong A W, Trotta R, Feroz F, Graff P and Hobson M P 2016 *ApJ* **824** 16 (*Preprint* 1602.02243)

[22] Kachelriess M, Moskalenko I V and Ostapchenko S S 2015 *ApJ* **803** 54 (*Preprint* 1502.04158)

[23] Urquhart J S, Figura C C, Moore T J T, Hoare M G, Lumsden S L, Mottram J C, Thompson M A and Oudmaijer R D 2014 *MNRAS* **437** 1791–1807 (*Preprint* 1310.4758)